Optimization of the adsorption of diclofenac by activated carbon and the acidic regeneration of spent activated carbon

Nevim Genç, Elif Durna and Ezgi Erkişi

ABSTRACT

Diclofenac sodium (DCF) is a non-steroidal anti-inflammatory drug. It has been classified as ecotoxic even at low concentrations. In this study, adsorption of DCF on coconut shell-based granular activated carbon (GAC) and regeneration of spent GAC with hydrochloric acid (HCl) were investigated. The results showed that GAC with heterogeneous surface structure adsorbs DCF endothermically with both chemical and physical forces. Adsorption and regeneration processes were optimized with Taguchi Experimental Design. The effects of all parameters affecting the adsorption and regeneration processes were determined by analysis of variance and Pareto analyses. DCF removal of 79.80% was obtained at optimum conditions and the most effective parameter was evaluated as GAC size. At optimum regeneration conditions, 6.85 mg DCF/g GAC adsorption capacity was found with an operating cost of €0.05 g GAC. The amount of HCl was the most effective parameter. It was determined that the regenerated GAC had an adsorptive capacity higher than the adsorptive capacity of the raw GAC during at least three regeneration cycles. Raw, spent and regenerated GACs were characterized by Fourier transform infrared spectrometry and scanning electron microscopy analysis.

Key words | activated carbon regeneration, DCF adsorption, Pareto analysis, process optimization, Taguchi Experimental Design

Nevim Genç (corresponding author)
Elif Durna
Ezgi Erkişi
Department of Environmental Engineering, Faculty of Engineering,
Kocaeli University,
41380, Kocaeli,
Turkey
E-mail: *ngenc@kocaeli.edu.tr*

HIGHLIGHTS

- At optimum adsorption conditions 79.8% DCF removal was obtained.
- With multi-response optimization for regeneration process, adsorption capacity of 6.847 mg DCF/g GAC with an experimental cost of €0.051 was found.
- The most effective parameters in adsorption and regeneration were found to be GAC size and HCl dosage, respectively.
- Regeneration capacity decreased by 47.1% after a total of 16 regeneration cycles.

GRAPHICAL ABSTRACT

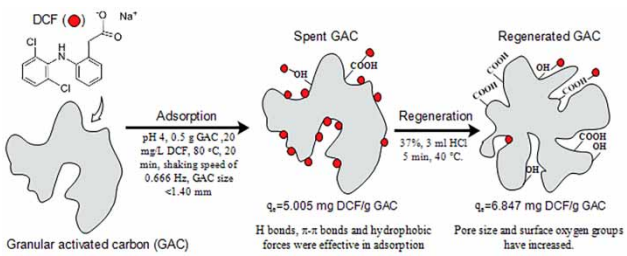

doi: 10.2166/wst.2020.577

INTRODUCTION

Micro-pollutants with a range of ng-μg/L and their metabolites in the aquatic environment, such as personal care products and pharmaceuticals, have unpredictable effects on the ecological system and human health (Zhuan & Wang 2020). Among pharmaceuticals, diclofenac sodium (DCF) is usually used as a non-steroidal anti-inflammatory drug. It has been classified as ecotoxic, hence it has recently been included in the list of primary pollutants by the EU (European Union) (Diaz-Angulo *et al.* 2020). DCF is a pollutant regularly found in aquatic environments, due to its high consumption rate (Sotelo *et al.* 2014). Micro-pollutants are generally not efficiently removed by conventional treatment processes due to their low biodegradability. DCF removal in sewage treatment plants is known to be only up to 21–40% (Zhang *et al.* 2008). Unfortunately, discharge standards are insufficient for monitoring such micro-pollutants (Kowalska *et al.* 2020). In order to increase the removal of such pollutants, conventional wastewater treatment plants should be improved with more effective technologies. The removal efficiencies obtained by some studied methods for removal of DCF are coagulation–membrane bioreactor (42±15.5%) (Park *et al.* 2018), combined ozonation–sonolysis (90–94%) (Fraiese *et al.* 2018), carbon-polymeric membrane (44%) (Nadour *et al.* 2019), biological degradation (10%) (Lee *et al.* 2019) and adsorption by activated carbon (above 90%) (Lee *et al.* 2019).

Among the methods used in wastewater treatment, the adsorption method has shown outstanding performance (Viotti *et al.* 2019). Adsorption is considered to be a flexible process in terms of both design and operation. Due to its excellent adsorbent properties, granular activated carbon (GAC) is used to separate the DCF. The use of carbon adsorbents obtained from renewable, low cost, abundant and natural products has been considered as a viable alternative. In DCF adsorption, adsorbents such as coconut shell (Purevsuren *et al.* 2016), *Moringa aleifera* pods (Viotti *et al.* 2019), cocoa shell (de Luna *et al.* 2017), olive stones (Larous & Meniai 2016) and Isabel grape bagasse (Antunes *et al.* 2012) were used. One limitation of adsorption by GAC is the depletion of adsorption pore sites. After the GAC saturated with the pollutant (i.e. spent), it can be replaced with fresh GAC, disposed of as solid waste, or regenerated for reuse (Huling *et al.* 2011; Hutson *et al.* 2012). Since adsorption is sometimes reversible, regenerating the adsorbent provides significant cost savings (Gil *et al.* 2019). The regeneration of GAC is a fundamental step in the sustainability of adsorption processes (Alvarez-Pugliese *et al.* 2019). Different methods for the regeneration of spent GAC have been developed, including thermal, chemical, microbiological and vacuum regeneration. Chemical and thermal regeneration techniques are commonly used for carbonaceous adsorbent regeneration. Chemical regeneration has emerged as an alternative to traditional thermal regeneration for reducing energy requirements and increasing regeneration efficiency (Salvador *et al.* 2015). Regeneration of GAC by chemical methods is an alternative method that can be performed *in situ* and on site (Hutson *et al.* 2012). Chemical regeneration can be defined as the desorption or decomposition of adsorbates using certain chemical reagents. In chemical regeneration, carbon attrition is not rapidly performed. In chemical methods, regeneration takes place through a chemical reaction or a pH change in the medium containing the GAC. Depending on the adsorbates are removed when the pH of the adsorbent surface changes. In chemical regeneration, mechanisms are extraction, pH changes, reaction/degradation and thermal desorption (Salvador *et al.* 2015). Traditionally, acid and alkaline chemicals are used for regeneration (Li *et al.* 2015).

Currently, there are few studies on GAC regeneration spent with pharmaceutical compounds. pH changes are often sufficient to displace the adsorption equilibria between the adsorbate and the adsorbent and promote desorption processes (Alvarez-Pugliese *et al.* 2019).

There is limited literature available on DCF adsorption by GAC and regeneration of DCF spent GAC. Therefore, this work investigated the DCF adsorption on coconut shell-based commercial GAC and regeneration of spent GAC. To determine the nature of the interaction between DCF and GAC, kinetic, isotherm and thermodynamic studies were performed. The adsorption process is optimized for high adsorptive capacity, while the regeneration process is optimized for high regenerative capacity at low operating cost. Optimization was carried out using the Taguchi Experimental Design. Optimization results of adsorption and regeneration will be used to evaluate the potential feasibility of processes.

METHODS

Diclofenac sodium ($C_{14}H_{10}C_{l2}NNaO_2$) was supplied by Abdi İbrahim Co. Properties of Diclofenac sodium are given in

Table 1. The coconut shell-based GAC used in the study (Tarkim-Carbon-200) was obtained from Tarkim-Carbon Co. in Turkey. The Brunauer–Emmett–Teller surface area, iodine content and dimensions of GAC are 1,100 m^2/g, 100 mg/g, and 1.41–2 mm, respectively. Hydrochloric acid (HCl) was obtained from Merck with a purity of 37% (12.06 N).

Experimental procedures

Experimental procedure of DCF adsorption

The batch experiments were carried out with solutions prepared by dilution of the DCF stock solution. For the kinetic experiments, studies were conducted by shaking 1 g GAC with 50 mL DCF solution (40 mg/L) at different time intervals (1–60 min) with the initial pH of 6.0 and at 20 °C. For sorption isotherms, 1 g GAC in a 50 mL DCF solution with concentrations ranging from 10 to 100 mg/L was shaken for 30 min at 20 °C with an initial pH of 6. To evaluate the thermodynamic parameters for DCF adsorption, 50 mL of DCF solution (40 mg/L) with 1 g activated carbon was equilibrated at different temperatures (293–333 K). After DCF adsorption of raw GAC, an aliquot of the supernatant was filtered from an 0.45 μm membrane filter, and the residual diclofenac analyzed using a UV–VIS spectrophotometer (Hach-Lange DR 5000) at a wavelength of 281 nm.

To optimize the parameters affecting the adsorption of DCF on GAC and the regeneration of spent GAC, Taguchi Experimental Design was used. The parameters and their levels affecting the adsorption process were determined as pH (4.0–9.0), GAC amount (0.1–0.5), initial concentration (20–40 mg/L), temperature (20–80 °C), adsorption time (5–10 min), shaking speed (0.666–1.000 Hz) and GAC size (size 1 is <1.40 mm and size 2 is 1.40–2.00 mm). The response parameter for the adsorption process was determined as DCF adsorption efficiency (%).

Experimental procedure of regeneration of spent GAC

DCF saturation of fresh GAC was accomplished with a concentrated DCF solution. The adsorption process was continued until the GAC could not adsorb the DCF molecules from the solution and the DCF concentration reached equilibrium in the solution. The spent GAC was mixed with the co-solution and the adsorption capacity of the regenerated GAC was determined. For regeneration experiments, the DCF spent GAC and co-solution (containing regenerating agent) were transferred to a glass beaker and exposed to regeneration by shaking the mixture. In order to determine the regeneration efficiency, experiments were carried out by shaking the mixture of regenerated GAC and DCF solution after GAC was washed several times with distilled water.

The parameters affecting the regeneration process were determined as HCl dosage (0.5, 3, 10 mL), regeneration time (5, 15, 30 min) and, temperature (20, 40, 80 °C). The levels of all parameters were determined by preliminary studies. The response parameter for the regeneration process was determined as the adsorption capacity (mg DCF/g GAC) and cost of regeneration process (€). Since more than one response parameter was selected for the optimization of spent GAC regeneration, the regeneration process was optimized as multi-parameter optimization. In the analysis, the responses were accepted as equal in weight. Energy and chemical consumption were taken into account in order to calculate the operating cost. The unit energy cost in the energy consumption of the magnetic stirrer was assumed to be €0.074/kWh. The unit cost of HCl was considered as €163/L.

Table 1 | Properties of DCF

Diclofenac sodium	pKa	LogKow	Water solubility (mg/L)	Molecular weight (g/mol)
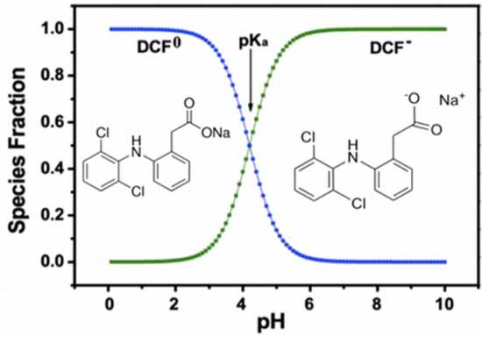	4.15	4.51	2.37 (at 25 °C)	296.147

The adsorption capacity of raw and regenerated GAC, q_e (mg/g), was calculated according to Equation (1):

$$q_e = \frac{(C_0 - C_e)}{m} V \quad (1)$$

where q_e is the amount of DCF adsorbed by GAC, C_0 and C_e refers to the initial and post-adsorption DCF concentrations (mg/L), V (L) is the solution volume and m (g) is the mass of GAC.

Surface functional groups on the GAC surface were analyzed with Perkin–Elmer Spectrum 100 FTIR, a Fourier transform infrared spectrometer (FTIR). The morphological and structural properties of the GACs were analyzed with a Philips XL30 FEG, which is a scanning electron microscope (SEM).

RESULTS AND DISCUSSION

Model fitting of adsorption process

Pseudo-first/second-order, intraparticle diffusion and Elovich kinetic models were used to examine the mechanism of the DCF adsorption process and to fit the kinetic data. The pseudo-first-order model is suitable for describing physisorption between adsorbed and adsorbent and specifies reversible interactions. The pseudo-second-order kinetic implies that the adsorption process takes place through strong chemical interaction forces between the adsorbent and the adsorbed (Viotti *et al.* 2019). The pseudo-second-order kinetic indicates that the adsorption capacity is proportional to the number of active zones filled on the adsorbent (Zhang *et al.* 2011). The pseudo-first-order and pseudo-second-order kinetic models may not be sufficient to explain the diffusion mechanism and the rate determination stage for adsorption. This can be explained by the intraparticle diffusion model (Kumar 2014). The intraparticle diffusion model can be used to define sequential mass transfer stages and to estimate the limiting step and the control mechanism in the adsorption kinetics (Maheshwari *et al.* 2013). Furthermore, the Elovich model can be successfully used to define the adsorption kinetics of the ion exchange system, to show that the adsorption process is a chemical process, especially an ion exchange process. In the Elovich model, an increase in α or a decrease in β increases the reaction rate (Genç & Dogan 2015).

Adsorption isotherms are required to gain some information about the adsorption mechanism, the surface properties and the tendency of adsorbent towards pollutants (Ghaedi & Kokhdan 2012). Adsorption isotherms can comprehensively explain how the adsorbate interacts with the adsorbents for the understanding of the nature of the interaction. In this study, some isotherms have been used. The Freundlich isotherm assumes the heterogeneity of the surface, and the adsorption occurs in regions with different adsorption energy (Maheshwari *et al.* 2013). It gives the relationship between equilibrium liquid and solid phase capacity. According to the Freundlich theory, the Freundlich constant (K_F) is the relative parameter of adsorption capacity and an n value greater than 1 indicates favourable adsorption (Wang *et al.* 2007), where $1/n$ is a measure of adsorption density and surface heterogeneity, and its approach to 0 represents an increase in heterogeneity (Moradi *et al.* 2013). The n value within $1 < n < 10$ indicates favourable adsorption and values outside the range indicates unfavourable adsorption (Liu & Wang 2013). The Langmuir adsorption model assumes that sorption is localized in a single layer and there is no interaction between the axes of the adsorbate molecules (Maheshwari *et al.* 2013). The Harkins–Jura isotherm model mainly explains multilayer adsorption and the presence of heterogeneous pore distribution on the adsorbent surface (Liu & Wang 2013). Halsey adsorption isotherm is suitable for multilayer adsorption, in particular, the fitting of the Halsey equation can be best used for heterotopous solids (Moradi *et al.* 2013). The isotherm and kinetic models used in this study are summarized in the Supplementary Material Table S1.

Thermodynamic analysis would be more appropriate to determine whether the process is governed by physisorption or chemisorption (Maheshwari *et al.* 2013). Thermodynamic parameters were given by the following equations (El-Shafey *et al.* 2012).

$$\Delta G^0 = -RT\ln K_d \quad (2)$$

where ΔG^0 indicates the standard free energy change (kJ/mol), T is the temperature (K), R is the universal gas constant (8.314 J/mol K) and K_d is the equilibrium constant.

$$K_d = \frac{C_o - C_e}{C_e} \quad (3)$$

$$\ln K_d = \frac{-\Delta H^0}{RT} + \frac{\Delta S^0}{R} \quad (4)$$

ΔH^0 and ΔS^0 are the change in entalphy and entrophy, respectively (Genç & Dogan 2015).

Isotherm, kinetic and thermodynamic studies

Adsorption kinetics provides extremely important information for understanding adsorption mechanisms (Viotti *et al.* 2019). Different types of kinetic models were examined for the adsorption of DCF on GAC. In kinetic studies, it can be said that DCF was in anionic form because the pH of the solution was about 6, which is above the pK value of DCF, which was 4.2. The kinetic rate constants and the linear regression correlation coefficient values for each model are shown in Table 2. From these results, it was observed that the linear plot for the pseudo-first-order kinetic model presents low correlation, showing a poor fit for the model; however, the linear plot for the pseudo-second-order kinetic model shows a better fitting with a high correlation coefficient value. The compatibility of DCF adsorption with pseudo-second kinetics indicates that it contains chemisorption as the rate-limiting mechanism, which occurs by electron sharing or exchange between DCF and GAC adsorption. In this study, the second-order kinetic constant k_2 and q_e were found to be 0.056 g/mg·min and 1.873 (mg/g), respectively. In the study conducted by Larous & Meniai (2016), they concluded that pseudo-second-order kinetics gives the best correlation for DCF adsorption with olive stone-based activated carbon. They found the k_2 and q_e kinetic constants as 1.5 g/mg·min and 3.10 mg/g, respectively. de Luna *et al.* (2017) also found that the pseudo-second-order kinetic is suitable for DCF adsorption with cocoa husk-based activated carbon. They found the k_2 and q_e kinetic constants as 0.39 g/mg·min and 5.67 mg/g, respectively. When adsorption occurs with chemical forces, the adsorbent and adsorbed substance form a chemical bond to share electrons (Mansour *et al.* 2018). It was determined that the $q_{e,cal}$ value calculated by the second-order kinetic expression is quite lower than the q_e value obtained experimentally (q_e, exp: 5.005 mg DCF/g GAC) and that k_2 depends on operating conditions. Also, k_2 relates to how quickly equilibrium is reached (Sekulic *et al.* 2019). In this study, the k_2 value is relatively low; therefore, the time required to reach equilibrium is relatively long.

Table 2 | Determined coefficients with kinetic and isotherm studies

Kinetic model	Constants
First-order kinetic	$k_1 = 0.004606$ (1/min), $q_e = 4.45$ (mg/g), $R^2 = 0.838$
Second-order kinetic	$k_2 = 0.056$ (g/mg·min), $q_e = 1.873$ (mg/g), $R^2 = 0.984$
Intraparticle diffusion	$C = 0.145$, $K_{diff} = 0.219$ (mg/g.min$^{1/2}$), $R^2 = 0.9445$
Elovich	$\alpha = 1.033$ (mg/g·min), $\beta = -3.195$ (g/mg), $R^2 = 0.721$
Isotherm	
Langmuir	$q_m = 6.76$ (mg/g), $K_L = 0.024$ (L/mg), $R^2 = 0.95$
Freundlich	$K_F = 0.243$ (mg/g)(1/mg)^n, $n = 1.37$, $R^2 = 0.961$
Harkins–Jura	$A = -0.197$, $B = 0.359$, $R^2 = 0.737$
Halsey	$n = -1.37$, $K_F = 6.96$, $R^2 = 0.961$
Thermodynamic	
293 (K)	$\Delta G^0 = 1.8849$ (kJ/mol), $\Delta H^0 = 19.15$ (kJ/mol), $\Delta S^0 = -0.0734$ (kJ/mol · K), $R^2 = 0.8381$
303 (K)	$\Delta G^0 = 3.6298$
313 (K)	$\Delta G^0 = 3.9580$
323 (K)	$\Delta G^0 = 4.7240$
333 (K)	$\Delta G^0 = 4.9217$

The Freundlich and Halsey isotherm models can be used for multilayer adsorption and heterogeneous surfaces with non-uniform distribution of adsorption heat. By comparing the R^2 values of the studied models from Table 2, it can be concluded that Freundlich and Halsey models fit better than others. In this study, the K_F coefficient for DCF was calculated as 0.243 (mg/g) (1/mg)^n. This coefficient is related to the adsorbent (Sekulic *et al.* 2019). Lach & Szymonik (2020) reported that in adsorption of DCF on commercial activated carbons, the K_F coefficient ranges from 26.02 to 9.17 mg/g. It was observed that the activated carbon used in this study has a very low affinity for DCF. In addition, $1/n$ value was found to be 1.37. The surface inhomogeneity of the adsorbent is rather low when $1/n$ values are closer to 0 (Lach & Szymonik 2020). The values of the thermodynamic parameters for the adsorption of DCF on GAC are also presented in Table 2. The negative values of change in ΔS^0 can be used to describe the randomness at the AC solution interface during the adsorption process (Kumar 2014). In addition, negative ΔS^0 indicates that the more ordered arrangement of dissolved molecules is shaped on the adsorbent surface (Wang *et al.* 2007).

The adsorption of DCF on GAC is an endothermic process, which is suggested by the positive value of the ΔH^0 (Moradi *et al.* 2013). Endothermic processes prefer higher temperatures across the external layer and within the pores of the adsorbent, which increases the diffusion rate. Also, ΔH^0 values higher than 20 kJ/mol are characteristic of the chemical adsorption process (Viotti *et al.* 2019). In this study, the ΔH^0 value was obtained as 19.14 kJ/mol. The absolute values of ΔH^0 in the range of 10–20 kJ/mol

indicate the π–π interaction, the van der Waals force and hydrogen the bonding, which corresponds to the physical adsorption process (Wang *et al*. 2007; El-Shafey *et al*. 2012). It can be said that the adsorption of DCF on GAC occurs with the effects of both physical and chemical forces.

Optimization of DCF adsorption and GAC regeneration processes

Optimization of DCF adsorption

The optimization study was carried out to determine the operating conditions that provide maximum DCF adsorption on GAC. All experimental data in the Taguchi Experimental Design and response parameter in terms of DCF adsorption efficiency (%) are shown in Table 3. The Taguchi Experimental Design should include operating conditions to ensure low, medium and high responses. If it was observed that any parameter had no effect on the yield in the preliminary experiments, it would not be included in the experimental design. Since the selected parameters had an effect on the responses in the preliminary experiments, the levels of these parameters were determined to have a low, medium and high effect on the responses.

The consistence of the model was confirmed by analysis of variance (ANOVA) with a F value of 91.99 and a *P*-value of less than 0.05. ANOVA results are shown in Table 4. A (pH) and F (shaking speed) parameters, which are not specified in the ANOVA table, were included in the error due to their insignificant effect on the response. Higher F values indicate that the models are significant. Model parameters with a *P*-value of less than 0.05 are considered to be significant. When the *P*-value is examined, it is seen that the model is significant for DCF adsorption. In addition, the parameters of GAC amount, temperature, adsorption time and GAC size were determined as important parameters affecting DCF adsorption.

In addition, Pareto analysis was performed in order to determine the effects of variables on the adsorption of DCF. Pareto analysis is a useful method of determining the significance of effects in order of magnitude and displaying the 5% significance threshold (t-value limit) and an additional threshold (Bonferroni limit) corrected for multiple tests.

Table 3 | The Taguchi Experimental Design of DCF adsorption on GAC

Run	A: pH	B: GAC amount (g)	C: Initial concentration (mg/L)	D: Temperature (°C)	E: Adsorption time (min)	F: Shaking speed (Hz)	G: GAC size*	Removal efficiency (%)
1	4.0	0.1	20	20	5	0.666	1	40.30
2	4.0	0.1	20	80	10	1.000	2	27.85
3	4.0	0.5	40	20	5	1.000	2	19.91
4	4.0	0.5	40	80	10	0.666	1	76.09
5	9.0	0.1	40	20	10	0.666	2	12.99
6	9.0	0.1	40	80	5	1.000	1	41.16
7	9.0	0.5	20	20	10	1.000	1	67.63
8	9.0	0.5	20	80	5	0.666	2	33.81

*For GAC size 1 refers to <1.40 mm and size 2 refers to 1.40–2.00 mm.

Table 4 | The ANOVA analysis of DCF adsorption on GAC

Source	Sum of squares	DF	Mean square	F value	*P*-value prob > F	Statement
Model	3,372.01	5	674.40	91.99	0.0108	Significant
B	705.94	1	705.94	96.29	0.0102	Significant
C	47.18	1	47.18	6.44	0.1265	
D	181.42	1	181.42	24.75	0.0381	Significant
E	304.71	1	304.71	41.56	0.0232	Significant
G	2,132.75	1	2,132.75	290.92	0.0034	Significant
Error	14.66	2	7.33			
Total	3,386.67	7				

The t-values of the bars represent the square root of the F values on the ANOVA. The parameters with the t-value on the Bonferroni line are defined as strictly significant, the parameters with the t-value between the Bonferroni line and the t-value limit are defined as potentially significant, and the parameters below the t-value limit line are defined as insignificant (Asem *et al*. 2018; Abdulredha *et al*. 2019). As seen in Figure 1, the most effective parameter for DCF adsorption on GAC was the GAC size. Potentially significant parameters were GAC amount, adsorption time and temperature. The initial concentration, pH and shaking speed were found as ineffective parameters in the adsorption of DCF on GAC. The parameters indicated by orange in the Pareto graph (see online version for colours) affect the adsorption positively and the parameters indicated by blue affect the adsorption negatively. For example, an increase in GAC size negatively affects DCF adsorption, whereas an increase in GAC amount, adsorption time and temperature parameters positively affects the DCF adsorption.

Supplementary Figure S1 shows the determined optimum experimental conditions for the DCF adsorption. The optimum conditions were obtained as pH 4.0, GAC amount of 0.5 g, initial concentration of 20 mg/L, temperature of 80 °C, adsorption time of 20 min, shaking speed of 0.666 Hz and GAC size of 1 (<1.40 mm). At optimum conditions, 79.8% DCF adsorption efficiency was obtained, which is higher than from all the adsorption efficiencies in the Taguchi Experimental Design. DCF adsorption efficiency predicted by the model was 79.06. The result obtained with the optimization experiment is within the 95% confidence interval in terms of model estimation.

Optimization of regeneration of spent GAC with HCl

In this study, the regeneration process of spent GAC with HCl was also optimized by the Taguchi Experimental Design. Operating cost of regeneration process and

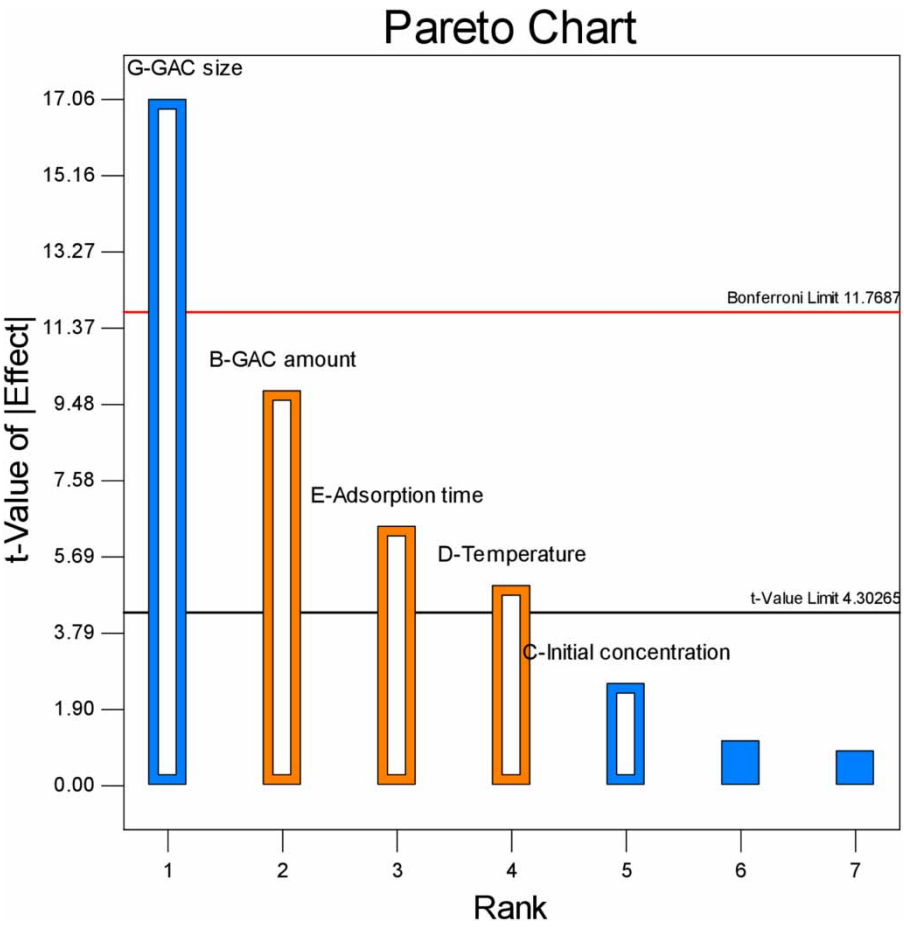

Figure 1 | Pareto analysis of DCF adsorption on GAC.

adsorptive capacity of GAC after regeneration were determined as response parameters. Hence, optimum regeneration conditions that will provide the low experimental cost and high adsorptive capacity of the spent GAC were determined by multi-response Taguchi Experimental Design analysis. For determining optimum regeneration conditions, HCl dosage, temperature and reaction time were determined as the parameters affecting the responses. Optimum operating conditions were determined to provide maximum adsorptive capacity and minimum operating cost simultaneously. Details of the multi-response Taguchi Experimental Design analysis are presented in Supplementary Materials.

The L9 Taguchi Experimental Design with experimental parameters, their levels and the obtained response values for the regeneration of spent GAC are shown in Table 5. The adsorptive capacity of raw GAC was found to be 5.005 mg DCF/g GAC.

ANOVA analysis was carried out to determine statistically important control parameters. Table 6 shows the results of ANOVA from the calculated MRSN values. In ANOVA, F and P (%) are useful for quantitative evaluation of parameter effects. Also, the factor with a high percentage contribution value has a greater effect on the response variable. According to ANOVA results, the amount of HCl is the most contributing parameter to the responses and has the greatest influence of 76.59%. Although the parameter of time is included in the error due to its very low contribution, the parameter of temperature has an influence of 5%.

The parameters effects on multi-response signal/noise (S/N) ratio (MRSN) are shown in Supplementary Figure S2. Overall mean value was calculated as 4.40. As shown in the Supplementary Figure S2., the optimum operating conditions for spent GAC regeneration are the second level of the A parameter, the first level of the B parameter and the second level of the C parameter. These conditions correspond to the HCl dose of 3 mL, a reaction time of 5 min and a temperature of 40 °C. At optimized conditions, 6.847 mg DCF/g GAC adsorption capacity was found with a experimental cost of €0.051. Total MRSN value of 7.26 was found with optimized conditions. The MRSN value predicted by the model was 7.28, while the confidence interval was found as ±3.52. Therefore, it can be said that the MRSN value obtained as a result of the optimum experiment remains within the confidence intervals.

Table 6 | The ANOVA analysis of DCF spent GAC regeneration

Paremeter	DF	Sum of square	Mean square	F value	Pure sum (P%)
A	2	24.235	12.118	7.416	76.59
B*	2	1.634	0.817	–	
C	2	3.139	1.569	0.960	5.09
Error	2	1.634	0.817	–	18.30
Total	8	29.507			100.00

*The parameter where the percentage contribution is <10% is considered as insignificant (Ramakrishnan & Karunamoorthy 2006). In this study, time parameter (B) is considered insignificant and it is included in the error term.

Effect of regeneration cycle on the adsorptive capacity of spent GAC

Depending on the properties of the adsorbate, regeneration takes place via a chemical reaction or a pH change in the medium containing GAC (Salvador *et al.* 2015). Acidic treatment of the GAC can affect adsorptive capacity through physical processes, including the breakdown of carbon surfaces, widening of micropores and a decline in GAC

Table 5 | The Taguchi experimental design of regeneration of DCF spent GAC

Run	A: HCl dosage (mL)	B: Regeneration time (min)	C: Temperature (°C)	Adsorptive capacity (q_e) (mg DCF/g GAC)	Experimental cost (€)	MRSN
1	0.5	5	20	4.976	0.00851	5.66
2	0.5	15	40	4.749	0.00854	5.25
3	0.5	30	80	3.659	0.00858	2.99
4	3	5	40	6.546	0.05101	6.96
5	3	15	80	5.293	0.05104	5.46
6	3	30	20	6.073	0.05108	6.44
7	10	5	80	8.369	0.17001	2.25
8	10	15	20	8.720	0.17004	2.30
9	10	30	40	8.800	0.17008	2.31

surface area (Karanfil & Kilduff 1999). The frequency of regeneration of GAC and its performance after each regeneration is very important for cost savings. Figure 2 shows the adsorption capacities as a function of regeneration cycle. During the first three regeneration cycles, the observed adsorbability of DCF on regenerated GAC was higher than raw GAC. This could be why the regeneration of hydrogen bond increased DCF adsorption after HCl regeneration. During the third to ninth regeneration cycles, there was no significant reduction in sorption. After 16 regeneration cycles, sorption was reduced by 47.1%. These results show that by HCl regeneration, the sorptive capacity of the GAC was protected and the useful life of the GAC was increased.

Characterization of the adsorbent

Raw, spent and regenerated GAC were characterized by SEM and FTIR spectroscopy. Figure 3 shows the SEM image of the raw, spent and regenerated GAC. The raw coconut shell-based GAC has a rough surface with small pores and cracks. Some salt particles appear to be scattered on the GAC surface due to the remaining phosphate or other metal compounds on the GAC after impregnation at the GAC production (Anisuzzaman *et al.* 2015). The DCF remains are observed on the SEM images of spent GAC. As seen in SEM images after regeneration, DCF residues on the adsorbent decreased.

Functional groups on the GAC surface were examined by FTIR spectroscopy. Figure 4 shows the various functional groups on raw, spent and regenerated activated carbons. Commercial activated carbons generally have lower structural complexity (Viotti *et al.* 2019).

When the FTIR spectrum of raw, spent and regenerated GAC were examined, it was observed that there were two distinct differences. The first is the presence of the peaks, which characterize DCF in the range of about 700–800 cm^{-1} in spent and regenerated GAC (Biorad Laboratories, n.d.). The peaks seen below 1,000 cm^{-1} belongs to the π (C–H) peaks. It can be said that the peaks in this region were formed by the adsorption of DCF by π–π interaction. These peaks cannot be removed by regeneration. The second important point observed with the FTIR spectrum is the change in the intensity of the peaks seen at 1,035 cm^{-1} (raw GAC), 1,072 cm^{-1} (regenerated GAC) and 1,082.6 cm^{-1} (spent GAC). The intensity of the peaks was ranked as regenerated GAC> raw GAC> spent GAC. The peaks at this range are probably associated with phenolic CO and OH, and primer alcohol–OH. The peaks in this region are caused by adsorption and desorption of DCF by electrostatic interaction.

The possible functional groups on the surface of raw, spent and regenerated GAC are presented in Table 7.

Possible DCF adsorption mechanism on carbon-based adsorbent may include: (1) H-bonding between the surface oxygen groups on carbon and DCF molecules, (2) π–π

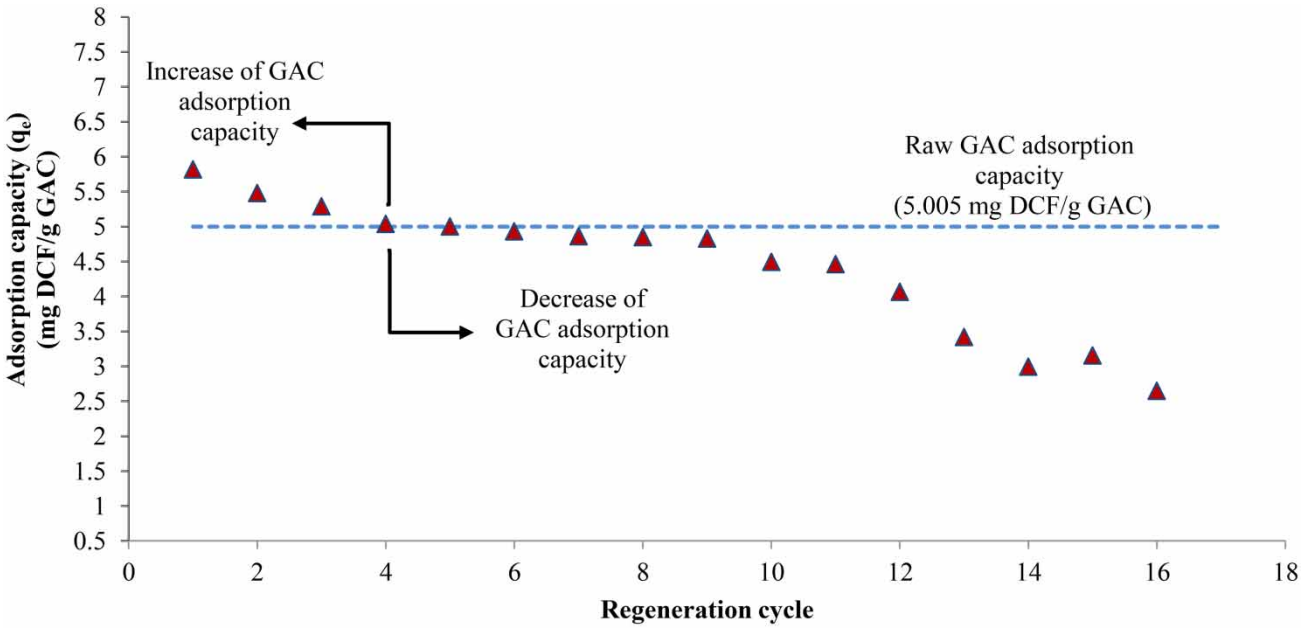

Figure 2 | Change of the adsorption capacity of regenerated GAC against the regeneration cycle.

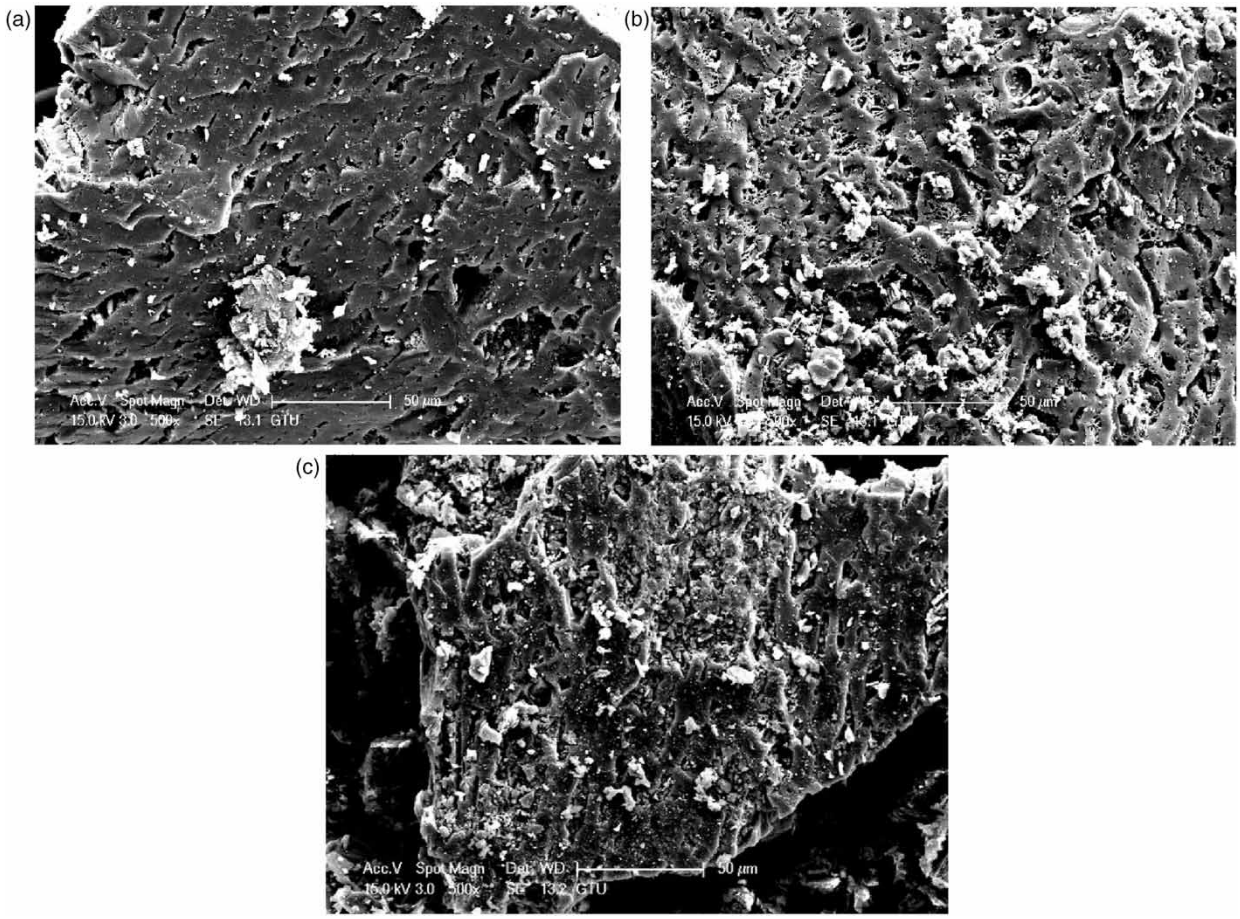

Figure 3 | SEM images of (a) raw, (b) spent and (c) regenerated GAC. Magnification power ×500.

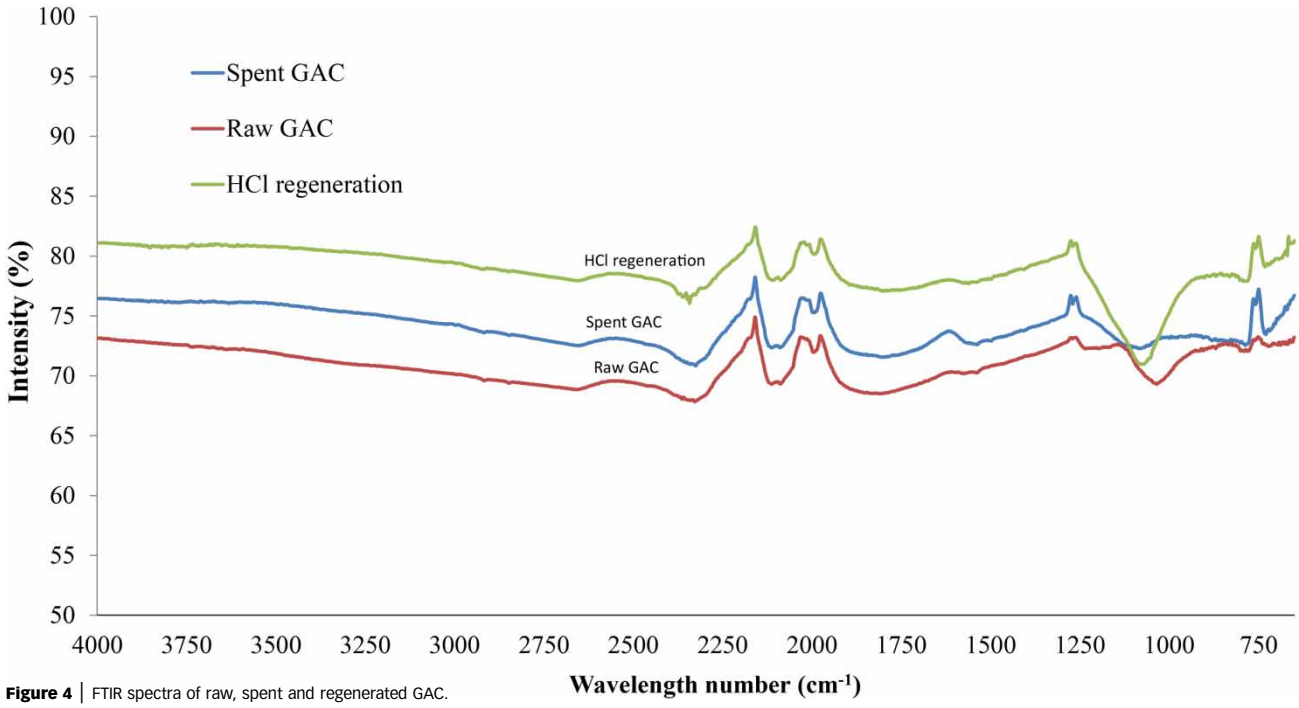

Figure 4 | FTIR spectra of raw, spent and regenerated GAC.

Table 7 | Possible functional groups and intensities of raw, spent and regenerated GAC

Wavelength (cm^{-1})	Possible functional groups	Raw GAC	Spent GAC	Regenerated GAC
723–801	C–Cl	Very weak	Strong	Strong
1,035–1,083	Primary alcohol –OH Phenolic CO and OH	Average	Weak	Strong
1,220	Phenolic –OH	Average	Weak	Weak
1,538–1,567	C=C aromatic C=O stretching of the carboxyl ion N–H vibration	Weak	Average	Weak
1,900–2,300	Methyl cellulose peaks Alkynes (C≡C)	Strong	Strong	Strong

interactions between the surface carbon (π–electron donor) and aromatic rings of DCF molecules (π–electron acceptors), (3) hydrophobic interactions (El Naga *et al.* 2019). When pH < 4.15, DCF species existed mainly in the form of organic acid. H-bonding interactions should dominate the mechanism. When pH > 6.5, DCF species existed mainly in the form of anions with $–COO^-$ group. Repulsion effect between both negatively charged DCF and GAC was expected (Wu *et al.* 2020). When the raw and spent GAC FTIR spectra are examined, it is seen that the C=C peak of the spent GAC shifts to 1,541 and 1,538 cm due to the π–π interaction in the adsorbent and adsorbate benzene ring (Jin *et al.* 2015). Figure 5 shows the possible adsorption mechanism of DCF on GAC.

CONCLUSION

In this study, the adsorption of DCF, which is one of the pharmaceuticals evaluated by the EU in the class of priority pollutants, with commercial coconut shell-based GAC and the regeneration of spent GAC were investigated. The study was carried out in four sections and the following results were obtained.

- The characterization of the nature of DCF adsorption by activated carbon was carried out. According to the ionic form of DCF in the aquatic solution, both physical and mainly chemical forces are effective in the adsorption DCF on GAC. The adsorption process of DCF on GAC was found to be compatible with the Freundlich and Halsey isotherm, which characterizes the heterogeneous surface structure and endothermic nature.
- The DCF adsorption process has been optimized by the Taguchi Experimental Design. The optimum conditions obtained were pH 4.0, 0.5 g of GAC, initial concentration of 20 mg/L, temperature of 80 °C, adsorption time of 20 min, shaking speed of 0.666 Hz and GAC size 1 (<1.40 mm). As a result of these verification experiment performed with these optimum conditions, DCF adsorption efficiency of 79.8% was obtained and this value is compatible with the model predicted value of 79.06% at 95% confidence level. All parameters effective in adsorption were optimized for maximum DCF adsorption efficiency. Based on the Pareto analysis and *P*-values, it was determined that the most effective parameter in the adsorption of DCF on GAC was GAC size. The parameters of GAC dosage, adsorption time and temperature parameters were also determined to have a

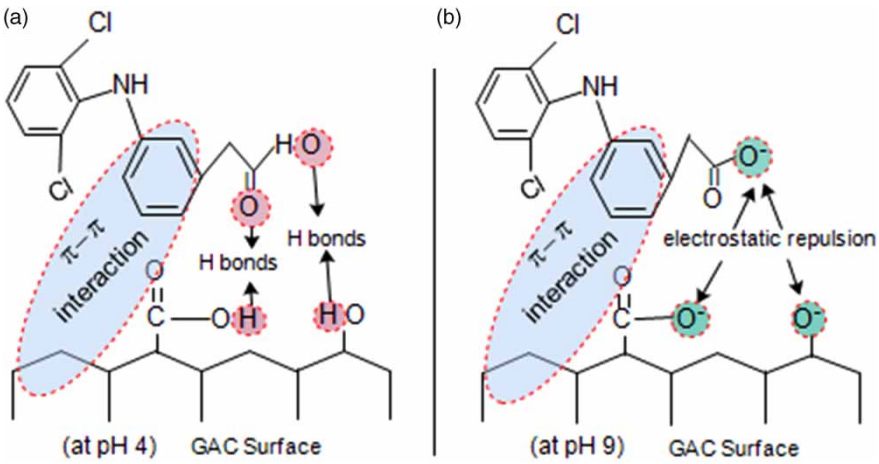

Figure 5 | Possible mechanism of DCF adsorption on GAC.

significant effect. During the adsorption process, π–π interaction, H-bonding and electrostatic repulsion interactions play an important role.

- Regeneration of DCF spent GAC with HCl was optimized for maximum adsorptive capacity at minimum cost simultaneously. The most effective parameter affecting the regeneration process was found to be HCl dosage with 75% effect. The optimum conditions were obtained as an HCl dose of 3 mL, the reaction time of 5 min and a temperature of 40 °C for the regeneration of spent GAC. As a result of the verification experiment carried out with the optimum conditions, adsorption capacity of 6.847 mg DCF/g GAC, experimental cost of €0.051 and MRSN of 7.26 was achieved. The MRSN value found is compatible with the model predicted value of 7.28 at 95% confidence level. When the effect of the regeneration cycle on the adsorptive capacity of the spent GAC was examined, it was found that at the end of a total of 16 regeneration cycles, there was a 47% reduction compared to the adsorptive capacity of raw GAC, which is 5.005 mg DCF/g GAC.
- DCF, an important microcontaminant, was removed with a high efficiency from water with a coconut shell-based GAC. Regeneration of depleted GAC with HCl increased the lifetime of GAC as well as adsorption capacity.

DATA AVAILABILITY STATEMENT

All relevant data are included in the paper or its Supplementary Information.

REFERENCES

Abdulredha, M. M., Hussain, S. A. & Abdullah, L. C. 2019 Separation emulsion via non-ionic surfactant: an optimization. *Processes* **7**, 382.

Alvarez-Pugliese, C. E., Acuña-Bedoya, J., Vivas-Galarza, S., Prado-Arce, L. A. & Marriaga-Cabrales, N. 2019 Electrolytic regeneration of granular activated carbon saturated with diclofenac using BDD anodes. *Diamond and Related Materials* **93**, 193–199.

Anisuzzaman, S. M., Joseph, C. G., Taufiq-Yap, Y. H., Krishnaiah, D. & Tay, V. V. 2015 Modification of commercial activated carbon for the removal of 2,4-dichlorophenol from simulated wastewater. *Journal of King Saud University-Science* **27**, 318–330.

Antunes, M., Esteves, V. I., Guégan, R., Crespo, J. S., Fernandes, A. N. & Giovanela, M. 2012 Removal of diclofenac sodium from aqueous solution by Isabel grape bagasse. *Chemical Engineering Journal* **192**, 114–121.

Asem, M., Nawawi, W. M. F. W. & Jimat, D. N. 2018 Evaluation of water absorption of polyvinyl alcohol-starch biocomposite reinforced with sugarcane bagasse nanofibre: optimization using two-level factorial design. *IOP Conference Series: Materials Science Engineering* **368**, 012005.

Biorad Laboratories. n.d. https://spectrabase.com/spectrum/IRvypsRL3jl (accessed 15 January 2020).

De Luna, M. D. G., Budianta, W., Rivera, K. K. P. & Arazo, R. O. 2017 Removal of sodium diclofenac from aqueous solution by adsorbents derived from cocoa pod husks. *Journal Environmental Chemical Engineering* **5**, 1465–1474.

Diaz-Angulo, J., Lara-Ramos, J., Mueses, M., Hernández-Ramírez, A., Puma, G. L. & Machuca-Martínez, F. 2020 Enhancement of the oxidative removal of diclofenac and of the TiO_2 rate of photon absorption in dye sensitized solar pilot scale CPC photocatalytic reactors. *Chemical Engineering Journal* **381**, 122520.

El Naga, A. O. A., El Saied, M., Shaban, S. A. & El Kady, F. Y. 2019 Fast removal of diclofenac sodium from aqueous solution using sugar cane bagasse-derived activated carbon. *Journal of Molecular Liquids* **285**, 9–19.

El-Shafey, E. S. I., Al-lawati, H. & Al-Sumri, A. S. 2012 Ciprofloxacin adsorption from aqueous solution onto chemically prepared carbon from date palm leaflets. *Journal of Environmental Science* **24**, 1579–1586.

Fraiese, A., Naddeo, V., Uyguner-Demirel, C. S., Prado, M., Cesaro, A., Zarra, T., Liu, H., Belgiorno, V. & Ballesteros Jr., F. 2018 Removal of emerging contaminants in wastewater by sonolysis, photocatalysis and ozonation. *Global NEST Journal* **21**, 98–105.

Genç, N. & Dogan, E. C. 2015 Adsorption kinetics of the antibiotic ciprofloxacin on bentonite, activated carbon, zeolite and pumice. *Desalination and Water Treatment* **53**, 785–793.

Ghaedi, M. & Kokhdan, S. N. 2012 Oxidized multiwalled carbon nanotubes for the removal of methyl red (MR): kinetics and equilibrium study. *Desalination and Water Treatment* **49**, 317–325.

Gil, A., Taoufik, N., García, A. M. & Korili, S. A. 2019 Comparative removal of emerging contaminants from aqueous solution by adsorption on an activated carbon. *Environmental Technology* **40**, 3017–3030.

Huling, S. G., Ko, S., Park, S. & Kan, E. 2011 Persulfate oxidation of MTBE- and chloroform-spent granular activated carbon. *Journal of Hazardous Materials* **192**, 1484–1490.

Hutson, A., Ko, S. & Huling, S. G. 2012 Persulfate oxidation regeneration of granular activated carbon: reversible impacts on sorption behavior. *Chemosphere* **89**, 1218–1223.

Jin, Z., Wang, X., Sun, Y., Ai, Y. & Wang, X. 2015 Adsorption of 4-*n*-nonylphenol and bisphenol-A on magnetic reduced graphene oxides: a combined experimental and theoretical studies. *Environmental Science & Technology* **49**, 9168–9175.

Karanfil, T. & Kilduff, J. E. 1999 Role of granular activated carbon surface chemistry on the adsorption of organic compounds. 1. Priority pollutants. *Environmental Science & Technology* **33**, 3217–3224.

Kowalska, K., Maniakova, G., Carotenuto, M., Sacco, O., Vaiano, V., Lofrano, G. & Rizzo, L. 2020 Removal of carbamazepine, diclofenac and trimethoprim by solar driven advanced oxidation processes in a compound triangular collector based reactor: a comparison between homogeneous and heterogeneous processes. *Chemosphere* **238**, 124665.

Kumar, P. S. 2014 Adsorption of Lead II ions from simulated waste water using natural waste: a kinetic, thermodynamic and equilibrium study. *Environmental Progress & Sustainable Energy* **33**, 174–181.

Lach, J. & Szymonik, A. 2020 Adsorption of diclofenac sodium from aqueous solutions on commercial activated carbons. *Desalination And Water Treatment* **186**, 418–429.

Larous, S. & Meniai, A.-H. 2016 Adsorption of Diclofenac from aqueous solution using activated carbon prepared from olive stones. *International Journal Hydrogen Energy* **41**, 10380–10390.

Lee, S. H., Kim, K.-H., Lee, M. & Lee, B.-D. 2019 Detection status and removal characteristics of pharmaceuticals in wastewater treatment effluent. *Journal of Water Process Engineering* **31**, 100828.

Li, Q., Qi, Y. & Gao, C. 2015 Chemical regeneration of spent powdered activated carbon used in decolorization of sodium salicylate for the pharmaceutical industry. *Journal of Cleaner Production* **86**, 424–431.

Liu, J. & Wang, X. 2013 Novel silica-based hybrid adsorbents: Lead(II) adsorption isotherms. *The Scientific World Journal* **1**, 897159.

Maheshwari, M., Vyas, R. K. & Sharma, M. 2013 Kinetics, equilibrium and thermodynamics of ciprofloxacin hydrochloride removal by adsorption on coal fly ash and activated alumina. *Desalination and Water Treatment* **51**, 7241–7254.

Mansour, F., Al-Hindi, M., Yahfoufi, R., Ayoub, G. M. & Ahmad, M. N. 2018 The use of activated carbon for the removal of pharmaceuticals from aqueous solutions: a review. *Reviews in Environmental Science and Biotechnology* **17**, 109.

Moradi, O., Fakhri, A., Adami, S. & Adami, S. 2013 Isotherm, thermodynamic, kinetics, and adsorption mechanism studies of Ethidium bromide by single-walled carbon nanotube and carboxylate group functionalized single-walled carbon nanotube. *Journal of Colloid and Interface Science* **395**, 224–229.

Nadour, M., Boukraa, F. & Benaboura, A. 2019 Removal of Diclofenac, Paracetamol and Metronidazole using a carbon-polymeric membrane. *Journal of Environmental Chemical Engineering* **7** (3), 103080.

Park, J., Yamashita, N. & Tanaka, H. 2018 Membrane fouling control and enhanced removal of pharmaceuticals and personal care products by coagulation-MBR. *Chemosphere* **197**, 467–476.

Purevsuren, B., Batbileg, S., Dabaajav, Y., Namkhainorov, D., Kuznetsov, P. N. & Kuznetsova, L. I. 2016 Composition and properties of coal from the Tsaydam Nuur deposit in Mongolia. *Solid Fuel Chemistry* **50**, 1–6.

Ramakrishnan, R. & Karunamoorthy, L. 2006 Multi response optimization of wire EDM operations using robust design of experiments. *Int. J. Adv. Manuf. Technol* **29**, 105–112.

Salvador, F., Martin-Sanchez, N., Sanchez-Hernandez, R., Sanchez-Montero, M. J. & Izquierdo, C. 2015 Regeneration of carbonaceous adsorbents. Part II: chemical, microbiological and vacuum regeneration. *Microporous and Mesoporous Materials* **202**, 277–296.

Sekulic, M. T., Boskovic, N., Slavkovic, A., Garunovic, J., Kolakovic, S. & Pap, S. 2019 Surface functionalised adsorbent for emerging pharmaceutical removal: adsorption performance and mechanisms. *Process Safety and Environmental Protection* **125**, 50–63.

Sotelo, J. L., Ovejero, G., Rodríguez, A., Álvarez, S., Galán, J. & García, J. 2014 Competitive adsorption studies of caffeine and diclofenac aqueous solutions by activated carbon. *Chemical Engineering Journal* **240**, 443–453.

Viotti, P. V., Moreira, W. M., dos Santos, O. A. A., Bergamasco, R., Vieira, A. M. S. & Vieira, M. F. 2019 Diclofenac removal from water by adsorption on *Moringa oleifera* pods and activated carbon: mechanism, kinetic and equilibrium study. *Journal of Cleaner Production* **219**, 809–817.

Wang, H. L., Fei, Z.-H., Chen, J.-L., Zhang, Q.-X. & Xu, Y.-H. 2007 Adsorption thermodynamics and kinetic investigation of aromatic amphoteric compounds onto different polymeric adsorbents. *Journal of Environmental Science* **19**, 1298–1304.

Wu, L., Du, C., He, J., Yang, Z. & Li, H. 2020 Effective adsorption of diclofenac sodium from neutral aqueous solution by low-cost lignite activated cokes. *Journal of Hazardous Materials* **384**, 121284.

Zhang, Y., Geißen, S. U. & Gal, C. 2008 Carbamazepine and diclofenac: removal in wastewater treatment plants and occurrence in water bodies. *Chemosphere* **73**, 1151–1161.

Zhang, C.-L., Qiao, G.-L., Zhao, F. & Wang, Y. 2011 Thermodynamic and kinetic parameters of ciprofloxacin adsorption onto modified coal fly ash from aqueous solution. *Journal of Molecular Liquids* **163**, 53–56.

Zhuan, R. & Wang, J. 2020 Degradation of diclofenac in aqueous solution by ionizing radiation in the presence of humic acid. *Seperation and Purification Technology* **234**, 116079.

First received 28 August 2020; accepted in revised form 17 November 2020. Available online 7 December 2020